



ORIGINAL RESEARCH

Gate-controlled series capacitor: A new methodology for mitigating sub-synchronous resonance in a series-compensated DFIG-based wind farm

Mohamed Abdeen¹  | Mahmoud A. El-Dabah¹ | Jose Luis Domínguez-García² |
Salah Kamel^{2,3} 

¹Department of Electrical Engineering, Faculty of Engineering, Al-Azhar University, Cairo, Egypt

²IREC Catalonia Institute for Energy Research, Sant Adrià de Besòs, Barcelona, Spain

³Department of Electrical Engineering, Faculty of Engineering, Aswan University, Aswan, Egypt

Correspondence

Salah Kamel, IREC Catalonia Institute for Energy Research, Sant Adrià de Besòs, 08930 Barcelona, Spain.
Email: skamel@aswu.edu.eg

Funding information

European Union's Horizon 2020 Research and Innovation Programme through the Marie Skłodowska-Curie Grant, Grant/Award Number: 801342; Government of Catalonia's Agency for Business Competitiveness (ACCIO)

Abstract

Series-compensated transmission lines can lead to a sub-synchronous resonance (SSR) phenomenon at high compensation levels, where the system lacks stability. Gate-controlled series capacitor (GCSC) is widely used to damp the SSR. Here, an effective and new methodology for damping the SSR is presented. The proposed method aims to alleviate the SSR phenomenon based on estimating both the frequency and the maximum value of the voltage magnitude signal rather than using the Proportional Integral controller. The appropriate turn-off angle corresponding to the maximum value of the voltage magnitude signal is applied to the GCSC on the condition that the estimated frequency of the voltage magnitude signal is within the range of the SSR frequency. If the estimated frequency of the voltage magnitude signal is out of the range of the SSR frequency, the steady-state turn-off angle (113°) is applied to the GCSC. The capability of the proposed method for damping the SSR under various compensation levels, various wind speeds, and sub-synchronous control interaction (SSCI) is validated by time-domain simulation and eigenvalue analysis. Compared to the presented latest method for SSR damping using GCSC, all the obtained results demonstrate that the oscillations converge faster when the proposed method is activated.

1 | INTRODUCTION

Electricity generation from renewable energy sources is growing too fast due to the scarcity of fossil fuels and increased demand. Wind energy is the most prevalent renewable energy source. Since wind farms are so far from the consumption places, a long transmission line is used to transfer the generated power. Series capacitor is inserted into the transmission line to increase the transferred power. The higher the compensation level (the lower the series capacitor), the more the transferred power. Unfortunately, a high compensation level can lead to the sub-synchronous resonance (SSR) phenomenon which affects the system stability [1, 2].

SSR phenomenon occurs because of the interaction between the series-compensated transmission line and the generator, leading to the existence of another frequency less than the fun-

damental frequency. It is called the electrical natural frequency [1]. Several research papers have been presented for damping the SSR phenomenon [3–9]. On the basis of the previous works, the SSR phenomenon can be damped by adding a supplemental damping controller (SDC) to the doubly fed induction generator (DFIG) controller or using a flexible AC transmission system (FACTS) [3, 7]. Gate-controlled series capacitor (GCSC) is widely used among the series FACTS devices because it is flexible, cheap, and simple [7, 9–11]. In reference [12], the SSR phenomenon was damped by GCSC. The measured active power is used as an input signal. The steady-state turn-off angle ($\gamma_0 = 113.5^{\circ}$) is summed with the output of the proportional gain to generate the turn-off angle which is used for SSR mitigation. However, this method cannot damp the SSR at high compensation levels or low wind speeds. In reference [13], the authors used a fuzzy logic controller to determine the

This is an open access article under the terms of the [Creative Commons Attribution-NonCommercial-NoDerivs](https://creativecommons.org/licenses/by-nc-nd/4.0/) License, which permits use and distribution in any medium, provided the original work is properly cited, the use is non-commercial and no modifications or adaptations are made.

© 2023 The Authors. *IET Renewable Power Generation* published by John Wiley & Sons Ltd on behalf of The Institution of Engineering and Technology.

proportional gain based on the error between the reference and measured active powers. Although the stability is improved, this method consumes a long time to dampen the SSR, as well as the system is still unstable at high compensation levels and low wind speeds. In references [7, 9], the authors proposed adding an SDC to the traditional method [13] for better damping. The wind speed is required to obtain the reference line current. The results proved the effectiveness and capability of this method for SSR damping at high compensation levels and low wind speeds. In reference [14], a fuzzy logic controller was proposed to compute the gain of SDC based on the wind speed and the error between the measured and reference line currents for transferring as much power as possible and damping the SSR phenomenon simultaneously. Since the GCSC is so far from the wind farm location, the use of local signals is more reliable than remote ones to avoid communication issues, ensure continuous operation, and achieve a lower cost. Here, an effective, simple, and new methodology for damping the SSR phenomenon is presented. The main contributions of this paper are as follows:

1. A new GCSC methodology for damping the SSR phenomenon based on estimating both the frequency and the maximum value of the voltage magnitude signal is proposed.
2. This method is effective, simple, and easy to be implemented in practice.
3. Local signal, voltage magnitude signal, is used as an input signal, leading to more reliability.
4. The wind speed signal is not required, unlike the traditional methods [7, 9], leading to better damping, and lower cost.
5. The time-domain simulations and eigenvalue analysis are conducted to demonstrate the robustness of the presented method for damping the SSR phenomenon.

The rest of this paper can be organized as follows: Section 2 describes the GCSC. Section 3 spotlights the proposed methodology for SSR damping. Section 4 shows the power system model. Section 5 gives the eigenvalue analysis. Section 6 presents the simulation results and discussions. Section 7 introduces a performance comparison between the GCSC and thyristor-controlled series capacitor (TCSC) based on the proposed method. Finally, the main outcomes of this research are summarized in Section 8.

2 | GATE-CONTROLLED SERIES CAPACITOR

GCSC consists of a fixed capacitor with a reactance (X_c) in parallel with a pair of gate turn-off (GTO) thyristors, as shown in Figure 1.

Based on the turn-off angle γ , the effective reactance of the GCSC can be calculated as [15, 16]:

$$X_{GCSC}(\gamma) = \frac{X_c}{\pi} (2\gamma - 2\pi - \sin(2\gamma)) \quad 90 < \gamma < 180 \quad (1)$$

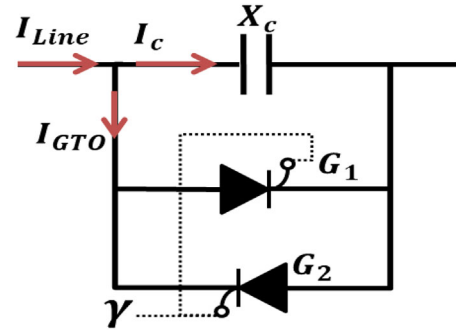


FIGURE 1 Basic gate-controlled series capacitor circuit. Here γ represents the turn-off angle, I_{Line} represents the line current, I_c represents the capacitor current, and I_{GTO} represents the GTO thyristor current.

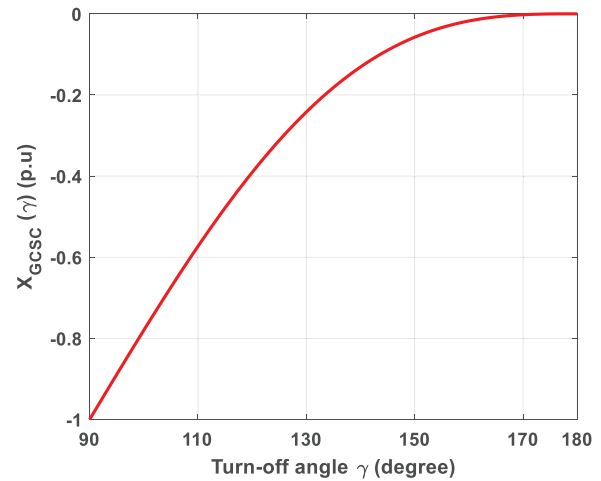


FIGURE 2 Gate-controlled series capacitor effective reactance in terms of the turn-off angle.

The turn-off angle γ is measured from the zero crossings of the line current. Figure 2 shows the effective reactance of the GCSC (X_{GCSC}) as a function of the turn-off angle γ .

It can be noted that as the γ changes from 90° to 180° , X_{GCSC} varies from X_c to zero. When the turn-off angle equals 90° , the effective reactance of the GCSC equals the fixed capacitor (X_c). That is to say, the GTO valve is opened ($I_{GTO} = \text{zero}$) and the capacitor is fully inserted into the circuit ($I_L = I_c$). Thus, the capacitor voltage is a maximum value. On the other hand, when the turn-off angle equals 180° , the effective reactance of the GCSC is equal to zero. Thus, the GTO valve is fully closed ($I_{GTO} = I_L$) and the capacitor is completely canceled ($I_c = \text{zero}$). Consequently, the capacitor voltage is equal to zero [16].

The GCSC waveforms for $\gamma = 120^\circ$ are shown in Figure 3, where the turn-off angle, pulses, capacitor voltage V_c , line current, GTO current, and capacitor current are plotted. As shown in Figure 3: (1) the GTO valve is closed automatically when the pulse is removed, (2) the capacitor current is equal to zero (value) when the GTO valve is closed (opened), and (3) the line current equals the sum of the capacitor current and GTO current.

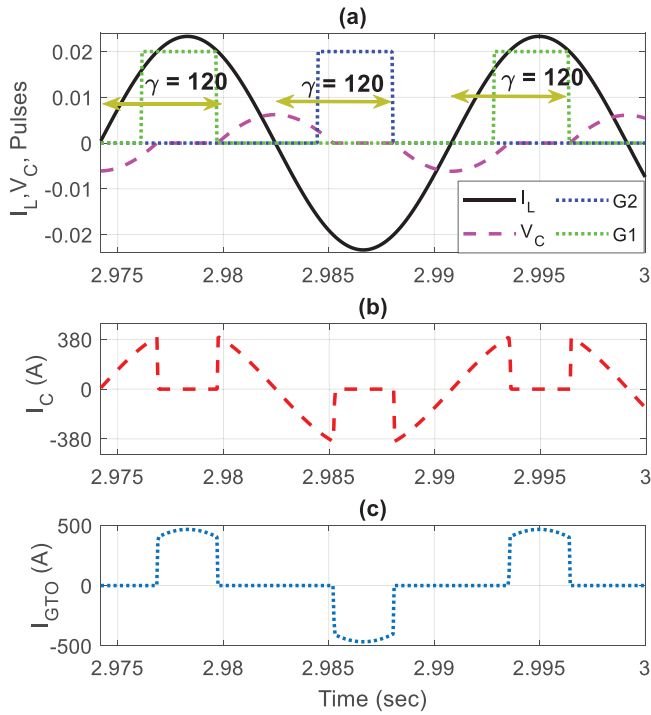


FIGURE 3 Gate-controlled series capacitor waveforms when turn-off angle = 120° . (a) Line current, capacitor voltage, and pulses. (b) Capacitor current. (c) GTO current.

Based on the turn-off angle, both the capacitor currents, GTO current, and capacitor voltage are determined.

3 | PROPOSED METHODOLOGY FOR SSR DAMPING

Since the GCSC is so far from the wind farm location, the communication link is needed to obtain the wind speed signal [7, 9], which affects the cost and the consumed time for mitigating the SSR. The proposed method's primary objective is to damp the SSR phenomenon based on estimating both the frequency and the maximum value of the voltage magnitude signal rather than using the PI controller. Figure 4 shows the scheme of the proposed method. In this study, the voltage magnitude signal is used as an input signal. It should be noted that any signal includes only one frequency when SSR occurs such as active power signal can be used as an input signal [17]. The proposed method can be described in three main parts as follows.

3.1 | Max. value estimation of the voltage magnitude signal

DC blocker: The voltage magnitude signal passes through the DC blocker for removing the DC component [17].

Switch: The DC blocker's output is fed to the "Switch" block to only pass the positive part V_s^+ , as shown in Figure 5a

Max. running resettable: The output of this block depends on the input value. If the input value is equal to zero, the output equals zero. When the input value is less (greater) than the previous value, the output is the previous (current) value, as shown in Figure 5b. The output of the max. running resettable block can be expressed using the following formula:

$$y_i = \begin{cases} v_{s(i)}^+ & v_{s(i)}^+ > v_{s(i-1)}^+ \\ 0 & v_{s(i)}^+ = 0 \\ v_{s(i-1)}^+ & v_{s(i)}^+ < v_{s(i-1)}^+ \end{cases} \quad (2)$$

where y_i is the output of the max. running resettable block, $v_{s(i-1)}^+$ is the previous value of the voltage, and $v_{s(i)}^+$ is the current value of the voltage.

Zero-order hold (ZOH): This block holds its input for a specific sample time (0.0045), as shown in Figure 5c.

Buffer: The output of ZOH is saved by the buffer block, as depicted in Figure 5d. The buffer's output can be expressed as:

$$\text{Buffer } r_{\text{output}} = \frac{J_1, J_2, \dots, J_i}{K} \quad (3)$$

where $K = 8$ and represents the buffer size.

2D Max: This block identifies the max value of the buffer's output for each output buffer size, as depicted in Figure 5e, and can be written as:

$$V_{\text{max}} = \max \left[\frac{J_1, J_2, \dots, J_i}{K} \right] \quad (4)$$

Lookup table: With increasing the compensation level or decreasing the wind speed, the amplitude of oscillation increases. Thus, the max value of the voltage magnitude signal increases. Based on the estimated max value of the voltage magnitude signal, the turn-off angle is generated. The higher the estimated max value of the voltage magnitude signal, the higher the turn-off angle. Thereby, the effective reactance of the GCSC decreases as shown in Figure 2, leading to decreasing the total compensation level. The values in the lookup table are determined based on the simulation tests.

3.2 | Frequency estimation of the voltage magnitude signal

To assure that this oscillation is because of the SSR phenomenon, the frequency of the voltage magnitude signal is also estimated to avoid erroneous judgments.

Sign: The DC blocker's output is fed to the "Sign" block to convert the sinewave to a square wave as shown in Figure 6b

Compare to zero: It is used to only pass the positive square wave as shown in Figure 6b.

Hit crossing: To avoid the zero crossings caused by the noise, the "Hit crossing" block is utilized to define the positive zero crossing of the sinewave according to the hit crossing offset (0.01).

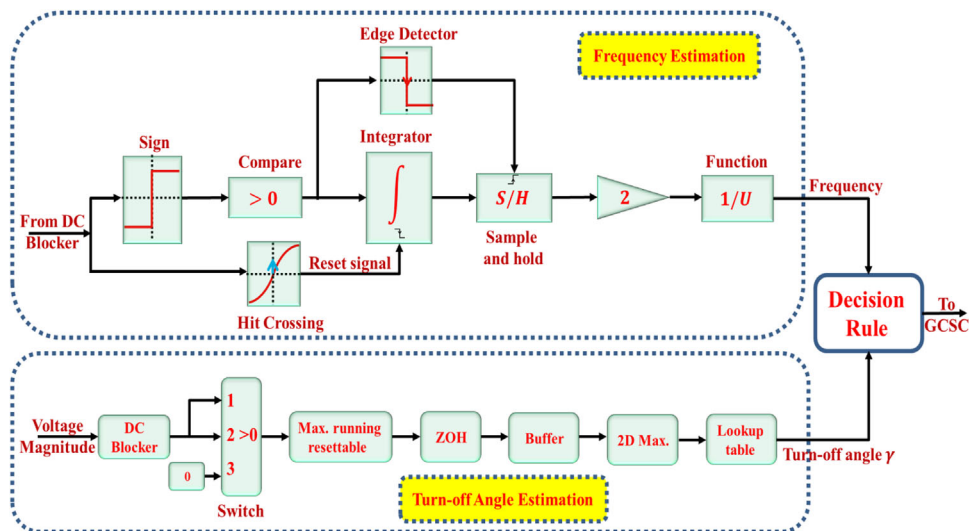
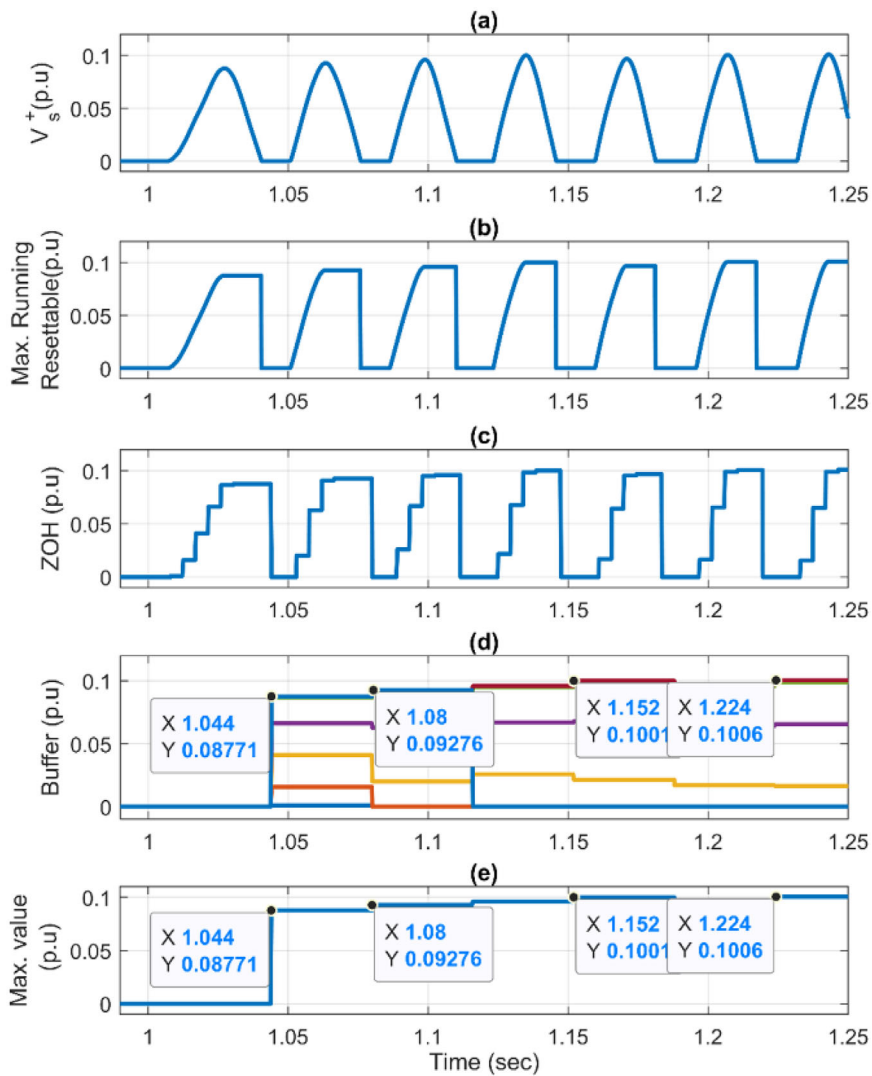


FIGURE 4 Proposed method scheme for sub-synchronous resonance damping.

FIGURE 5 Max. value estimation of the voltage magnitude signal. (a) Positive part of voltage magnitude signal, (b) Max. Running Resettable, (c) Zero order hold, (d) Buffer, and (e) Max. value of voltage magnitude signal.



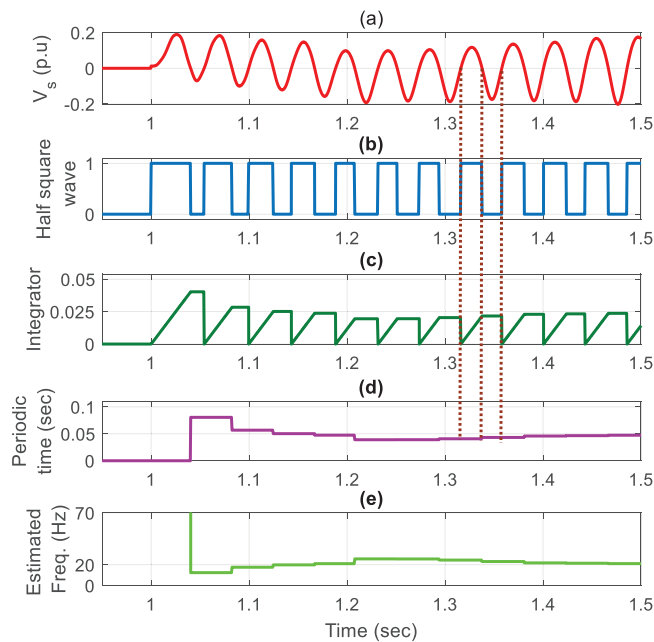


FIGURE 6 Frequency estimation of the voltage magnitude signal. (a) Voltage magnitude signal, (b) Half square wave, (c) Integrator, (d) Periodic time, and (e) Estimated frequency.

Integrator: It is used to convert the positive square wave to a sawtooth wave, as shown in Figure 6c. The “Hit crossing” block is used to reset the integrator at each positive zero crossing, as shown in Figures 4 and 6c.

Sample and hold: It stores the data of the sawtooth wave in a specific time to obtain the maximum value. It should be noted that the output of the “S/H” block is the half-cycle time. Thus, the output is multiplied by two to obtain the periodic time, as shown in Figure 6d.

Edge detector: It is used to apply an impulse to the “S/H” block when the value of the half-square wave changes from 1 to 0. This impulse is responsible for resetting the “S/H” block.

Function: The frequency of the voltage magnitude signal can be estimated according to the following equation, as shown in Figure 6e:

$$f = \frac{1}{\text{Periodic time}} \quad (5)$$

where periodic time is the time between two positive or negative zero crossings.

3.3 | Decision rule

If the estimated frequency of the voltage magnitude signal is within the range of the SSR frequency (15% to 90% of synchronous frequency [60 Hz]), the estimated turn-off angle corresponding to the maximum value of the voltage magnitude signal is applied to the GCSC. On the other hand, if the estimated frequency of the voltage magnitude signal is out of

TABLE 1 Sub-synchronous resonance mode at different compensation levels and 9 m/s wind speed.

K%	Without controller	Traditional method [9]	Proposed method
35	$-0.52 \pm j218$	$-5.2 \pm j217$	$-5.21 \pm j217$
45	$1.23 \pm j198$	$-4.8 \pm j197$	$-4.81 \pm j197$
55	$2.85 \pm j180$	$-3.5 \pm j179$	$-3.52 \pm j179$
65	$4.42 \pm j164$	$-2.1 \pm j163$	$-2.12 \pm j163$

the range of the SSR frequency, the steady-state turn-off angle (113°) is applied to the GCSC. The steady-state turn-off angle is chosen based on reference [12].

4 | POWER SYSTEM MODEL

The power system model is modified from the first Benchmark model to analyse the performance of the proposed method for alleviating the SSR phenomenon, as illustrated in Figure 7. This model has been widely used in many research works for SSR studies [3, 7–9, 17, 18]. In this system, a 100 MW DFIG-based offshore wind farm is connected to the infinite bus through a series-compensated transmission line. The 100 MW wind farm is made up of 67 wind turbine units, where the power rating of each unit is 1.5 MW. The DFIG has a rated voltage of 575 V and a frequency of 60 Hz. The model parameters are tabulated in reference [3].

5 | EIGENVALUE ANALYSIS

Eigenvalue consists of real and imaginary parts ($\lambda = \sigma \pm j\omega$). The real part refers to stability, where the system is stable (unstable) if the real part is negative (positive). The imaginary part refers to the oscillation frequency ($f = \omega/2\pi$). The damping ratio can be calculated in terms of the real and imaginary parts of the eigenvalue $= \frac{-\sigma}{\sqrt{\sigma^2 + \omega^2}}$.

At different compensation levels and constant wind speed (Table 1), it can be observed that without a controller, the system is unstable for $K = 45\%$, $K = 55\%$, and $K = 65\%$. The higher the compensation level, the lower the system stability. Whereas the system is stable with the traditional and proposed methods at different compensation levels. Compared to the traditional method [9], the stability is improved slightly when the proposed method is activated, especially at higher compensation levels ($K = 55\%$, and $K = 65\%$).

At variable wind speeds and constant compensation level (Table 2), it is clear that the stability is improved with increasing the wind speed. Without a controller, the system is unstable for $V_w = 7 \frac{m}{s}$, $V_w = 8 \frac{m}{s}$, and $V_w = 9 \frac{m}{s}$. Although the stability is improved with the traditional method, the system is still unstable for $V_w = 7 \frac{m}{s}$. The system is more stable when the proposed method is in use at variable wind speeds, especially at lower wind speeds.

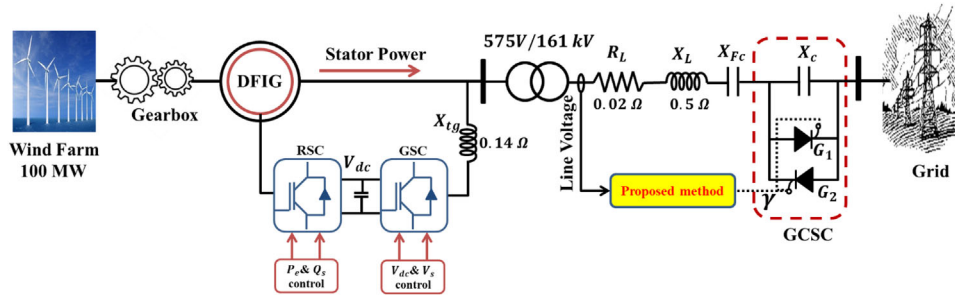


FIGURE 7 The study system.

TABLE 2 Sub-synchronous resonance mode at variable wind speeds and 50% compensation level.

V_w	Without controller	Traditional method [9]	Proposed method
7	$4.4 \pm j191$	$0.4 \pm j188$	$-5.5 \pm j186$
8	$2.9 \pm j189$	$-2.2 \pm j186$	$-5.9 \pm j184$
9	$2 \pm j188$	$-4.73 \pm j185$	$-4.74 \pm j183$

6 | SIMULATION RESULTS AND DISCUSSIONS

To prove the proposed method’s capability for damping the SSR phenomenon, it is examined under various wind speeds, compensation levels, and sub-synchronous control interaction (SSCI). Furthermore, the presented method’s performance is compared with the presented latest method [9] for SSR damping using GCSC to validate its effectiveness and robustness. The dynamic responses of the active power P_e , and the dc-link voltage V_{dc} from the DFIG wind turbine are plotted. In this study, the fixed series capacitor (X_{Fc}) represents 70% of the total compensation level, whereas the GCSC capacitor (X_c) represents 30% of the total compensation level.

6.1 | Various compensation levels

Before $t = 15$ s, the system is stable because of the lower compensation level. Then, at $t = 15$ s, the compensation level is increased to 45%, 55%, and 65%, as shown in Figures 8, 9, and 10, respectively. All the obtained simulation results with 9 m/s wind speed.

These observations can be extracted from Figures 8–10:

1. The system is unstable without a controller. On the other hand, the traditional method and the proposed method can dampen the SSR, as shown in Figures 8–10.
2. When the proposed method is in use, the SSR phenomenon is completely damped after 1, 1.5, and 2 s for $K = 45\%$, $K = 55\%$, and $K = 65\%$, respectively. In other words, the higher the compensation level, the longer the SSR damping time.

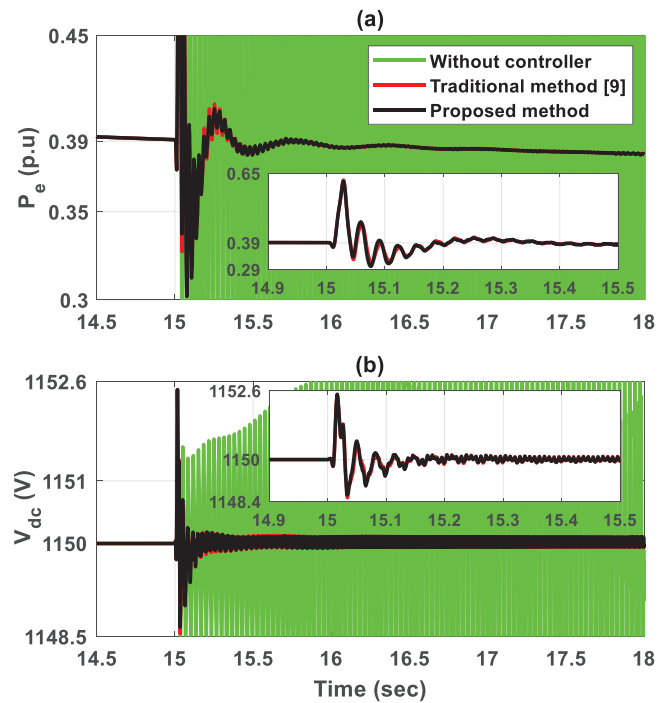


FIGURE 8 Dynamic response of DFIG at a wind speed of 9 m/s and compensation level of 45%. (a) active power, and (b) dc-link voltage.

3. Although the traditional method [9] and the proposed method can dampen the SSR in all studied cases, less oscillation amplitude is achieved by the proposed method, especially at higher compensation levels.
4. It can be noted that the eigenvalue analysis listed in Table 1 is consistent with the time-domain simulation.
5. Both the active power and dc-link voltage signals prove that there is no effect on the DFIG controller by the proposed method.

6.2 | Various wind speeds

As is well known, the system becomes more unstable as the wind speed decreases [1]. In this subsection, the simulation is carried out when the wind speed equals 7, 8, and 9 m/s for a constant compensation level ($K = 50\%$), as shown in

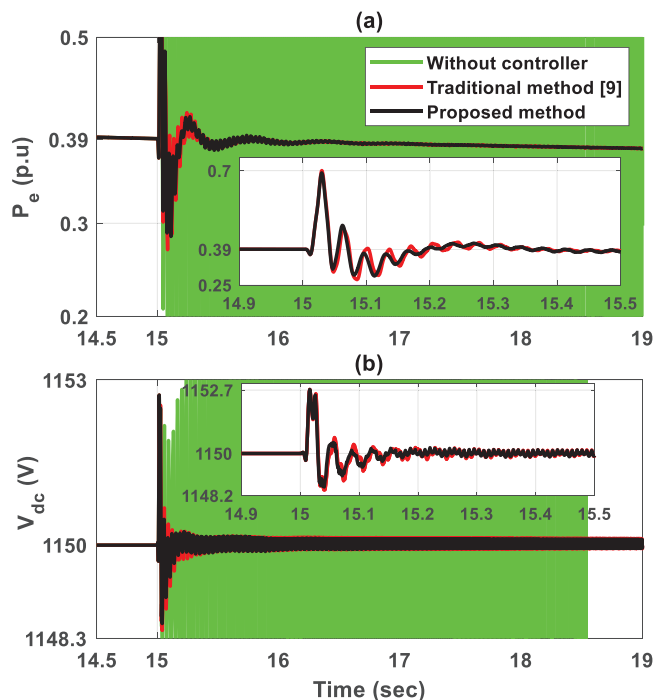


FIGURE 9 Dynamic response of DFIG at a wind speed of 9 m/s and compensation level of 55%. (a) active power, and (b) dc-link voltage.

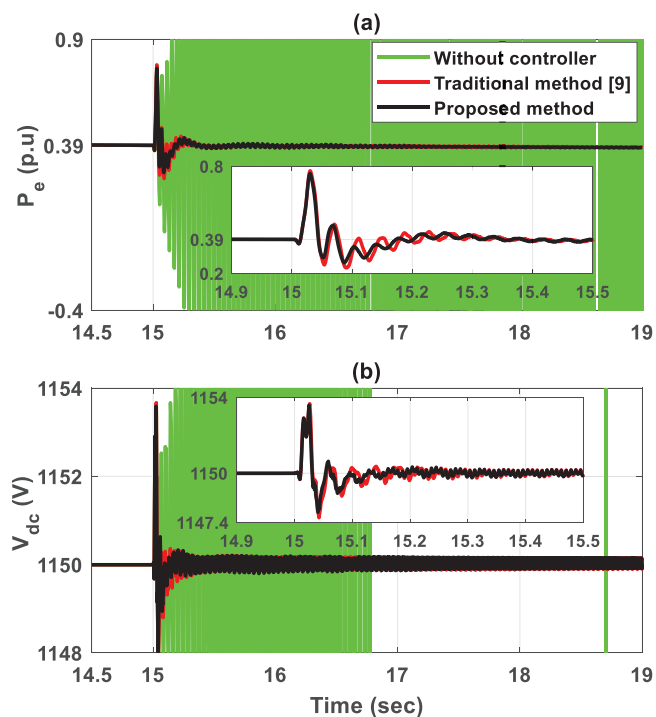


FIGURE 10 Dynamic response of DFIG at a wind speed of 9 m/s and compensation level of 65%. (a) active power, and (b) dc-link voltage.

Figures 11, 12, and 13, respectively. Initially, the system is stable. Then, at $t = 15$ s, K is increased to 50% in all studied cases.

As shown in these figures:

1. Without a controller, the system lacks stability in all studied cases. It can be observed that the lower the wind speed, the lower the system stability.
2. Figure 11 shows that the traditional method cannot dampen the SSR at the lowest wind speed (7 m/s). On the other hand, the proposed method can dampen the SSR successfully.
3. Compared to the traditional method, the best performance has been achieved by the proposed method, where the SSR is damped faster at various wind speeds.
4. The simulation results by MATLAB/Simulink confirm the eigenvalue analysis given in Table 2.

6.3 | SSCI

The interplay between DFIG controllers and series-compensated transmission lines causes SSCI. To analyse the performance of the proposed method with SSCI, a low wind speed, 7 m/s, and a three-phase-to-ground-fault are applied at $t = 15$ s for 200 ms with high compensation levels (i.e., $K = 60\%$, and $K = 65\%$), as shown in Figures 14 and 15. The following notes can be concluded from Figures 14 and 15.

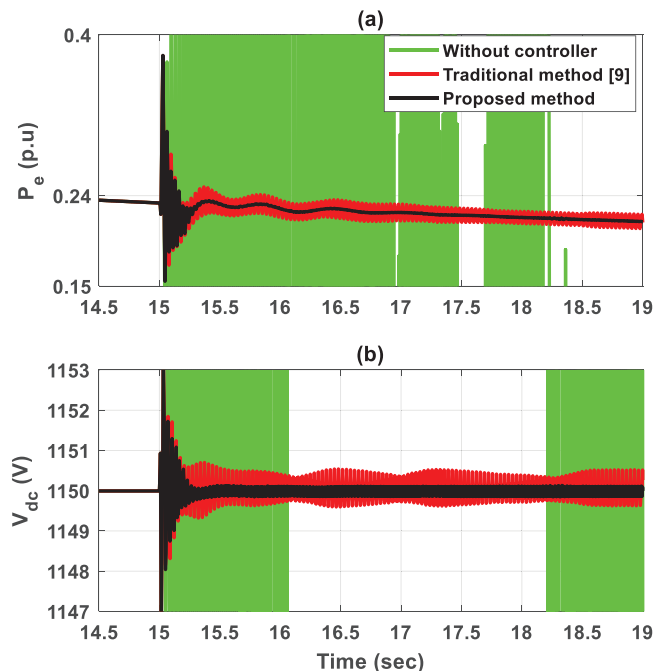


FIGURE 11 Dynamic response of DFIG at a wind speed of 7 m/s and compensation level of 50%. (a) active power, and (b) dc-link voltage.

1. Without a controller, the system is unstable in all studied cases. It can be noted that the SSCI is more severe than increasing compensation levels or decreasing wind speeds.
2. It can be observed that the oscillation's amplitude is lower and less time is needed for damping the SSR when the

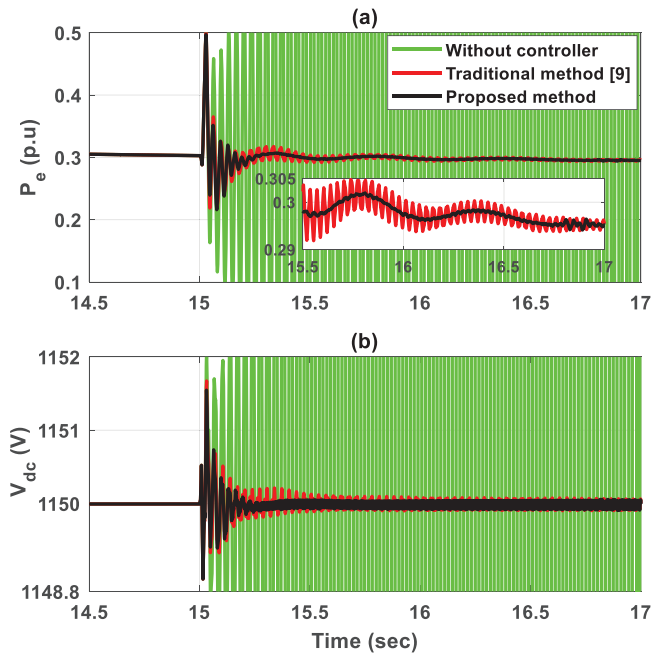


FIGURE 12 Dynamic response of DFIG at a wind speed of 8 m/s and compensation level of 50%. (a) active power, and (b) dc-link voltage.

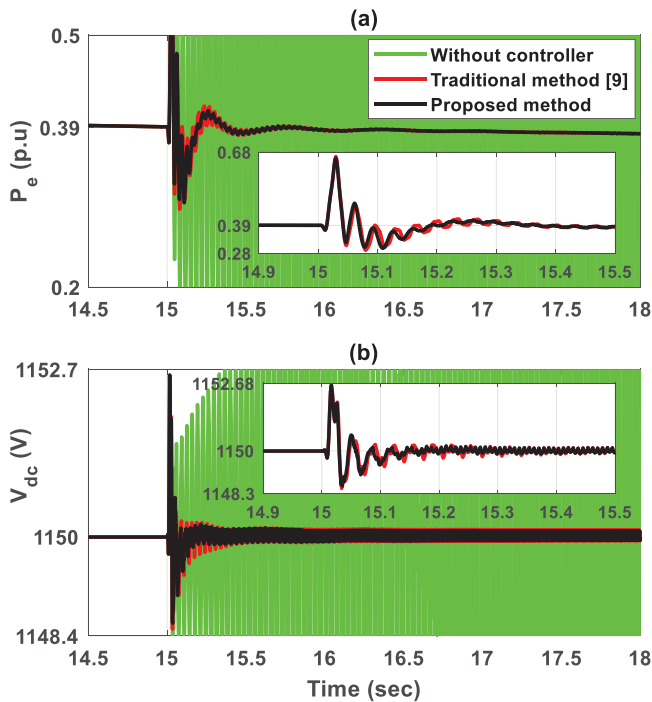


FIGURE 13 Dynamic response of DFIG at a wind speed of 9 m/s and compensation level of 50%. (a) active power, and (b) dc-link voltage.

proposed method is in use compared to the traditional method.

3. The results prove the robustness and effectiveness of the proposed method for damping the SSR under the worst cases of SSCI, especially in comparison to the traditional method.

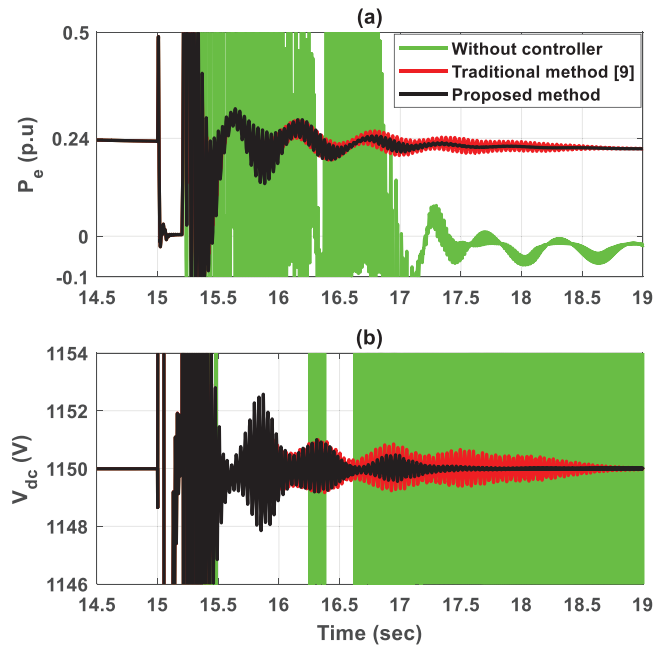


FIGURE 14 Dynamic response of DFIG (sub-synchronous control interaction) at a wind speed of 7 m/s and compensation level of 60%. (a) active power, and (b) dc-link voltage.

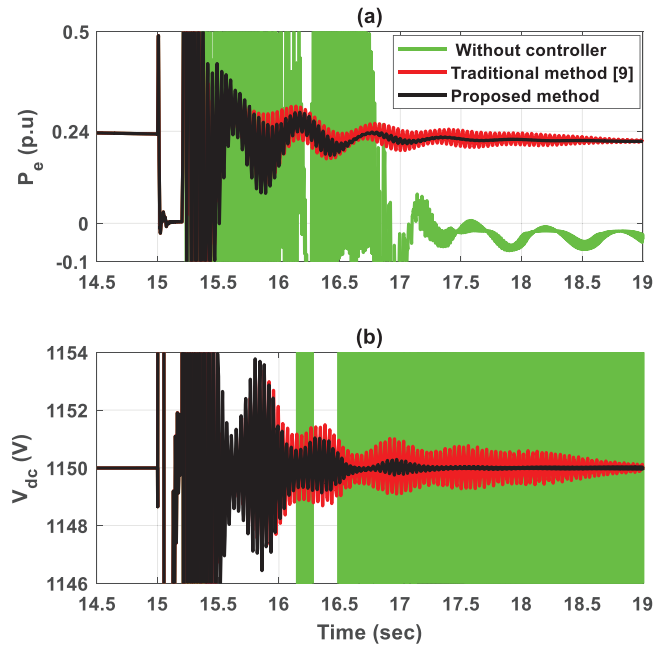


FIGURE 15 Dynamic response of DFIG (sub-synchronous control interaction) at a wind speed of 7 m/s and compensation level of 65%. (a) active power, and (b) dc-link voltage.

7 | PERFORMANCE COMPARISON BETWEEN THE GCSC AND THYRISTOR-CONTROLLED SERIES CAPACITOR BASED ON THE PROPOSED METHOD

Here, the performance of the proposed method with GCSC, and with TCSC is investigated at 8 m/s wind speed and 50%

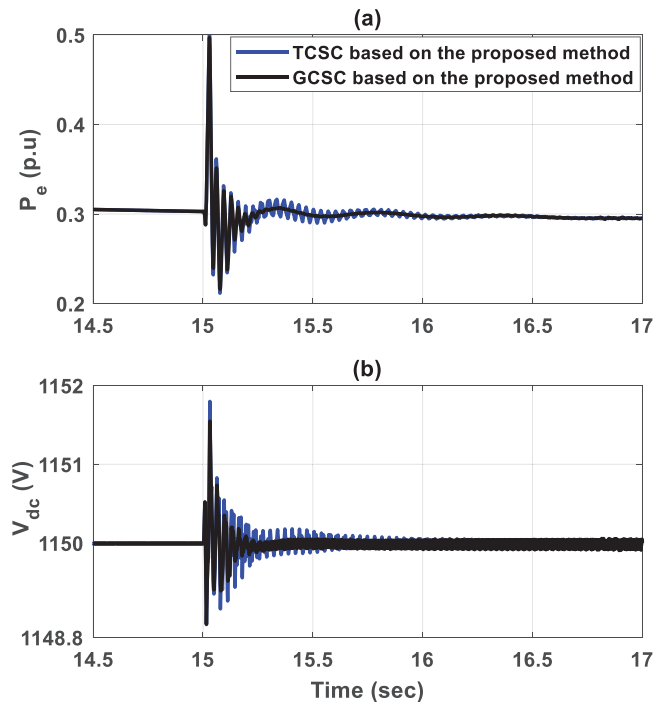


FIGURE 16 Performance comparison between the gate-controlled series capacitor and thyristor-controlled series capacitor based on the proposed method at 8 m/s wind speed and 50% compensation level. (a) active power, and (b) dc-link voltage.

compensation level. Both the DFIG active power and the dc-link voltage are plotted, as shown in Figure 16. The simulation results prove that the performance of the proposed method with GCSC is better than that of the TCSC, where the oscillation is damped after around 0.4 s with GCSC whereas it is damped after 1.5 s with TCSC.

8 | CONCLUSION

This paper proposed a simple, effective, and new approach for generating the turn-off angle of the GCSC based on estimating the max value of the voltage magnitude signal. To assure that this oscillation is because of the SSR phenomenon, the frequency of the voltage magnitude signal is also estimated. The generated turn-off angle is applied to the GCSC when the frequency of the voltage magnitude signal is within the range of SSR frequency. Otherwise, the steady-state turn-off angle (113°) is applied to the GCSC. The proposed method was tested with the prevailing types in a series-compensated DFIG-based wind farm (different wind speeds, different compensation levels, and SSCI). Moreover, a performance comparison between the GCSC and TCSC based on the proposed method was carried out for SSR damping. The results proved: (1) that the system is more stable and less time is required to mitigate the SSR when the proposed method is activated in all studied cases. (2) The superiority of the GCSC over TCSC for SSR damping, where a shorter time is achieved with GCSC, compared to TCSC. Furthermore, the proposed method is simple to imple-

ment in real-world wind farms because no remote signal (wind speed) is required.

AUTHOR CONTRIBUTIONS

Mohamed Abdeen: Conceptualization; methodology; software; writing—original draft. **Mahmoud A. El-Dabah:** Formal analysis; methodology; supervision; validation. **José Luis Domínguez-García:** Conceptualization; investigation; supervision; writing—review and editing. **Salah Kamel:** Conceptualization; investigation; software; writing—review and editing.

ACKNOWLEDGEMENTS

This project has received funding from the European Union's Horizon 2020 research and innovation programme under Marie Skłodowska-Curie grant agreement No. 801342 (Tecniospring INDUSTRY) and the Government of Catalonia Agency for Business Competitiveness (ACCIO).

CONFLICT OF INTEREST STATEMENT

The authors declare no conflicts of interest

DATA AVAILABILITY STATEMENT

The data that support the findings of this study are available from the corresponding author upon reasonable request.

ORCID

Mohamed Abdeen  <https://orcid.org/0000-0001-5273-0118>

Salah Kamel  <https://orcid.org/0000-0001-9505-5386>

REFERENCES

- Abdeen, M., Li, H., Kamel, S., et al.: A recent analytical approach for analysis of sub-synchronous resonance in doubly-fed induction generator-based wind farm. *IEEE Access* 9, 68888–68897 (2021)
- Xie, X., Zhang, X., Liu, H., et al.: Characteristic analysis of subsynchronous resonance in practical wind farms connected to series-compensated transmissions. *IEEE Trans. Energy Convers.* 32(3), 1117–1126 (2017)
- Abdeen, M., Li, H., Mohamed, M.A.E.H., et al.: Sub-synchronous interaction damping controller for a series-compensated DFIG-based wind farm. *IET Renew. Power Gener.* 16(5), 933–944 (2022)
- Abdeen, M., Emran, A., Moustafa, A., et al.: Investigation on TCSC parameters and control structure for SSR damping in DFIG-based wind farm. In: *12th International Renewable Energy Congress (IREC)*, pp. 1–5. IEEE, New Jersey (2021)
- Wu, X., Wang, M., Shahidehpour, M., et al.: Model-free adaptive control of STATCOM for SSO mitigation in DFIG-based wind farm. *IEEE Trans. Power Syst.* 36, 5282–5293 (2021)
- Leon, A.E., Amodeo, S., Mauricio, J.M.: Enhanced compensation filter to mitigate subsynchronous oscillations in series-compensated DFIG-based wind farms. *IEEE Trans. Power Delivery* 36, 3805–3814 (2021)
- Mohammadpour, H.A., Ghaderi, A., Santi, E.: Analysis of subsynchronous resonance in doubly-fed induction generator-based wind farms interfaced with gate-controlled series capacitor. *IET Gener. Transm. Distrib.* 8(12), 1998–2011 (2014)
- Piyasinghe, L., Miao, Z., Khazaei, J., et al.: Impedance model-based SSR analysis for TCSC compensated type-3 wind energy delivery systems. *IEEE Trans. Sustain. Energy* 6(1), 179–187 (2014)
- Mohammadpour, H.A., Santi, E.: Modeling and control of gate-controlled series capacitor interfaced with a DFIG-based wind farm. *IEEE Trans. Ind. Electron.* 62(2), 1022–1033 (2014)
- de Souza, L.F.W., Watanabe, E.H., da Rocha Alves, J.E.: Thyristor and gate-controlled series capacitors: A comparison of components rating. *IEEE Trans. Power Deliv.* 23(2), 899–906 (2008)

11. Emarloo, A.A., Changizian, M., Shoulaie, A.: Application of gate-controlled series capacitor to mitigate subsynchronous resonance in a thermal generation plant connected to a series-compensated transmission network. *Int. Trans. Electr. Energy Syst.* 30(12), e12673 (2020)
12. de Jesus, F.D., Watanabe, E.H., de Souza, L.F.W., et al.: SSR and power oscillation damping using gate-controlled series capacitors (GCSC). *IEEE Trans. Power Deliv.* 22(3), 1806–1812 (2007)
13. Pahlavani, M.R.A., Mohammadpour, H.A.: Damping of sub-synchronous resonance and low-frequency power oscillation in a series-compensated transmission line using gate-controlled series capacitor. *Electr. Power Syst. Res.* 81(2), 308–317 (2011)
14. Mohamed, A., El-Banna, S.H.A., Elgohary, S., et al.: Adaptive fuzzy supplementary controller for SSR damping in a series-compensated DFIG-based wind farm. *IEEE Access* 11, 1467–1476 (2023)
15. Padiyar, K.R.: *FACTS controllers in power transmission and distribution*. New Age International, Delhi (2007)
16. Hingorani, N.G., Gyugyi, L.: *Understanding FACTS: Concepts and technology of flexible AC transmission systems*. IEEE Press, New York (2000)
17. Abdeen, M., Li, H., Jing, L.: Improved subsynchronous oscillation detection method in a DFIG-based wind farm interfaced with a series-compensated network. *Int. J. Electr. Power Energy Syst.* 119, 105930 (2020)
18. Chowdhury, M., Shafiullah, G.: SSR mitigation of series-compensated DFIG wind farms by a nonlinear damping controller using partial feedback linearization. *IEEE Trans. Power Syst.* 33(3), 2528–2538 (2017)

How to cite this article: Abdeen, M., El-Dabah, M.A., Domínguez-García, J.L., Kamel, S.: Gate-controlled series capacitor: A new methodology for mitigating sub-synchronous resonance in a series-compensated DFIG-based wind farm. *IET Renew. Power Gener.* 17, 2638–2647 (2023). <https://doi.org/10.1049/rpg2.12776>